ChemComm

Accepted Manuscript

This article can be cited before page numbers have been issued, to do this please use: Y. Yuan, W. Wu, S. Xu and B. Liu, *Chem. Commun.*, 2017, DOI: 10.1039/C7CC01093A.

This is an Accepted Manuscript, which has been through the Royal Society of Chemistry peer review process and has been accepted for publication.

Accepted Manuscripts are published online shortly after acceptance, before technical editing, formatting and proof reading. Using this free service, authors can make their results available to the community, in citable form, before we publish the edited article. We will replace this Accepted Manuscript with the edited and formatted Advance Article as soon as it is available.

You can find more information about Accepted Manuscripts in the author guidelines.

Please note that technical editing may introduce minor changes to the text and/or graphics, which may alter content. The journal's standard Terms & Conditions and the ethical guidelines, outlined in our author and reviewer resource centre, still apply. In no event shall the Royal Society of Chemistry be held responsible for any errors or omissions in this Accepted Manuscript or any consequences arising from the use of any information it contains.

View Article Online
DOI: 10.1039/C7CC01093A

ChemComm

RSCPublishing

COMMUNICATION

Biosensor based on Self-Clickable AIEgen: A Signal Amplification Strategy for Ultrasensitive Immunoassay†

1. Cite this: DOI:10.1039/x0xx00000x

Youyong Yuan,[a,‡] Wenbo Wu,[a,‡] Shidang Xu,[a] and Bin Liu*[,a,b]

Received 00th January 2012,
Accepted 00th January 2012

DOI: 10.1039/x0xx00000x

www.rsc.org/

A signal amplified fluorogenic ELISA based on self-clickable fluorogen with aggregation-induced emission characteristics (AIEgen) as substrate was developed for ultrasensitive immunoassay.

Highly sensitive detection of protein biomarkers is of great importance to clinical decisions.[1] Enzyme-linked immunosorbent assay (ELISA), the most widely used immunoassay, has been extensively used for protein biomarker detection in laboratory research and clinical diagnosis due to its superior selectivity arising from the high specificity of antigen-antibody recognition.[2] The conventional ELISA mainly employs an enzyme conjugated antibody as a biocatalyst to hydrolyze the substrate such as 3,3′,5,5′-tetramethylbenzidine (TMB) or *p*-nitrophenyl phosphate (pNPP) into a colored product and the signal change is used to quantify the analyte.[3] Although the colorimetric method is simple and effective, it suffers from poor stability of the substrate and moderate sensitivity which is unable to analyze ultralow levels of analytes. To tackle these issues, fluorogenic ELISAs using organic dyes or fluorescent nanoparticles as the signal reporter were developed in recent years by taking advantages of the higher sensitivity of fluorescence signals relative to absorbance changes.[4] Most of the current fluorescent immunoassays either work on complicated signal generation mechanisms or rely on extensive synthesis of the fluorescent dyes/nanomaterials and antibody conjugates to replace the enzymatic labeling of antibody in traditional ELISA.[4] Such modifications may also lose the intrinsic signal amplification of enzymatic reactions.[5] To further enhance the detection sensitivity and assay simplicity, it is thus of great interest to develop a facile fluorogenic ELISA that could take advantages of both the enzymatic amplification of colorimetric ELISA,[4d] and the fluorescent signal amplification. This can be achieved through incorporation of a new signal reporting substrate into an existing colorimetric ELISA platform containing commercially available enzyme conjugates.

As a unique fluorogenic process, fluorogens with aggregation-induced emission characteristics (AIEgens) have recently gained increasing attention as a versatile and potent tool for sensing and imaging of diverse analytes including ions,[6] pH,[7] gas,[8] biomolecules,[9] and different processes, such as self-assembly.[10] Opposite to traditional fluorogens that show the notorious aggregation-caused quenching (ACQ) in aggregates, AIEgens are non-emissive in molecularly dissolved state but become highly emissivein aggregated state. The mechanism of AIE has been rationalized to be the restriction of intramolecular motionsin aggregated state and prohibition of energy dissipation *via* non-radiative channels.[11] The AIE-based biosensors possess advantages of improved signal output, low background interference and resistance to photo bleaching.[12] The unique properties of AIEgens have offered excellent opportunities for the development of assays for highly sensitive analyte detection.

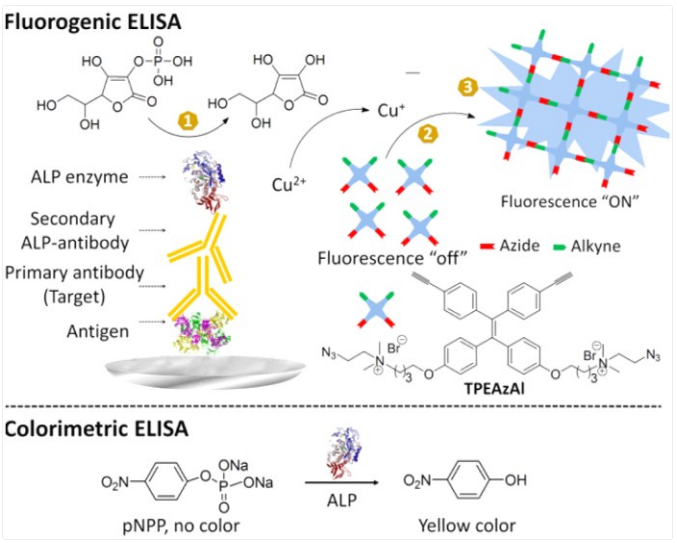

Figure 1. Schematic illustration of the working principle of the alkaline phosphatase (ALP)-triggered click reaction and fluorescence turn-on of TPEAzAl for fluorogenic ELISA. The conventional colorimetric ELISA using pNPP as substrate is also shown for comparision.

In this contribution, we develop a fluorogenic ELISA based on self-clickable TPEAzAl as substrate,which improves the sensitivity and stability for the immunoassay (Figure 1). TPEAzAl has good water solubility with negligible fluorescence in aqueous solution. It consists of an iconic AIEgen tetraphenylethene (TPE) as the core, which is functionalized with two alkyne and two azide groups. Once it undergoes cross-linking by click reaction to form aggregates, the AIE process is activated with fluorescence turn-on. The overall sensitivity of this fluorogenic ELISA is guaranteed due to several amplification processes: (1) Alkaline phosphatase can dephosphorylate ascorbic acid-phosphate to generate ascorbic acid (AA) which can reduce Cu^{2+} to Cu^{+}.[13] (2) The formed Cu^{+} can initiate click reactions between the alkyne- and azide groups of TPEAzAl to form polymer aggregates. (3) The click-induced fluorescence turn-on can further amplify the signal output. Compared with the conventional colorimetric ELISA using pNPP as substrate, the fluorogenic ELISA shares the same platform and the enzyme-labeled antibody, but uses TPEAzAl as substrate, which could take advantages of both enzymatic reactions and AIE based fluorescent signal amplification to enable ultrasensitive detection of various analytes.

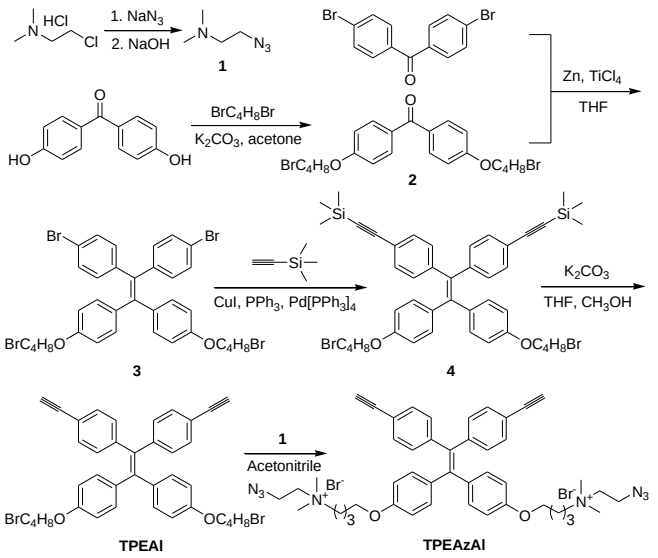

Scheme 1. Synthetic route to TPEAl and TPEAzAl.

The substrate, an azide- and alkyne dual-functionalized water-soluble TPEAzAl was synthesized according to the reaction routes shown in Scheme 1. Compound 1 was first obtained by treating 2-chloro-*N*,*N*-dimethylethanamine hydrochloride with sodium azide and further neutralized with sodium hydroxide. Treatment of 4,4'-dihydroxybenzophenone with an excess amount of 1,4-dibromobutane in basic condition afforded compound 2, which then underwent a McMurry coupling reaction with 4,4'-dibromobenzophenone to generate intermediate compound 3. The palladium-catalyzed Sonogashira coupling reaction between compound 3 and (trimethylsilyl)acetylene afforded compound 4. The trimethylsilyl groups were further de-protected by treatment with K_2CO_3, thereby furnishing the intermediate product TPEAl. Further reaction between TPEAl and excess amount of compound 1 in acetonitrile afforded the desired product of TPEAzAl. TPEAzAl and the intermediates were well characterized by NMR and mass spectroscopies (Figures S1-S9).

We first investigated the photophysicalproperties of TPEAl and TPEAzAl. The absorption maximum of TPEAl is 355 nm (Figure S10). The photoluminescence (PL) spectra of TPEAl in water and dimethyl sulfoxide (DMSO) mixtures at different water fractions (f_{water}) were studied and the results are shown in Figure 2A. TPEAl is faintly fluorescent in its benign solvent (DMSO) as the molecularly dissolved state can consume the energy through free molecular motion, which favors nonradiative decay.[11a] However, with gradual increase of water (poor solvent) fractions, TPEAl becomes highly emissive with an emission maximum at 530 nm, showing a characteristic AIE phenomenon. At the f_{water} of 99%, the fluorescence intensity at 530 nm is about 48-fold stronger than that in DMSO. This fluorescence enhancement should be due to the formation of aggregates which restrict the intramolecular motion to activate the AIE process. The formation of aggregates at the f_{water} of 99% was confirmed by dynamic light scattering (DLS) study (Figure S11A). Next, we studied the optical properties of TPEAzAl. As shown in Figure S10, TPEAzAl shows an absorption profile similar to that of TPEAl. As TPEAzAl is soluble in both water and DMSO, hexane (poor solvent) and isopropyl alcohol (benign solvent) mixture were applied to study its AIE characteristics. As shown in Figure 2B, TPEAzAl is faintly fluorescent in isopropyl alcohol but becomes highly emissive when the f_{hexane} is above 80% and the aggregation formation is also confirmed by DLS study (FigureS11B), indicating that TPEAzAl is also AIE-active. Although TPEAl and TPEAzAl show similar absorption profiles, their emission spectra in water are totally different. The PL spectra of TPEAl and TPEAzAl in DMSO/PBS buffer (v/v = 1/99) are shown in Figure 2C, TPEAl shows bright green fluorescence while TPEAzAl is almost non-emissive, indicating that TPEAzAl has low background signal, which is desirable for biosensing. The fluorescence intensity of TPEAzAl remains weak in aqueous media with different ionic strength or in the presence of proteins (Figures S12 and S13).

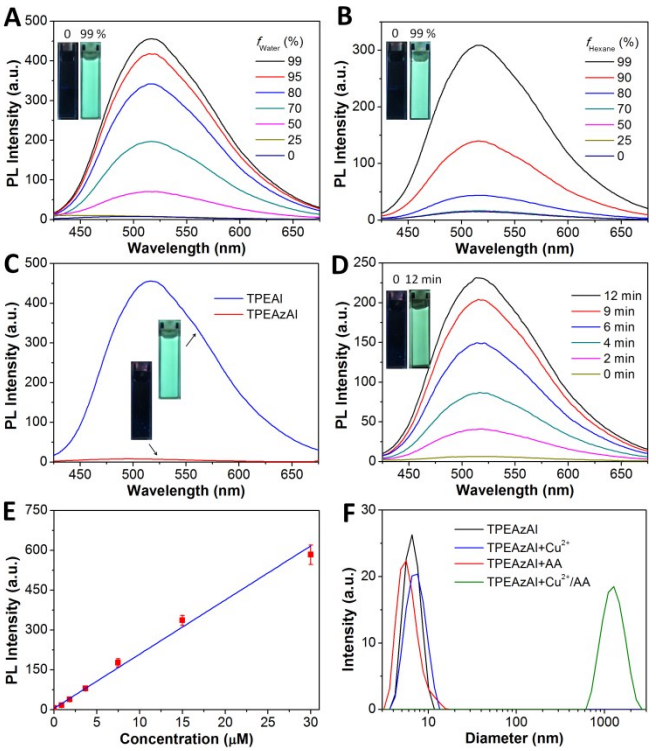

Figure 2. (A) Photoluminescence (PL) spectra of TPEAl (10 μM) in DMSO/water mixtures with different fractions of water (f_{water}). (B) PL spectra of TPEAzAl (10 μM) in isopropyl alcohol/hexane mixtures with different fractions of hexane (f_{hexane}). (C) PL spectra of TPEAl and TPEAzAl in DMSO/PBS mixtures (v/v = 1/99). (D) Time-dependent PL change of TPEAzAl (10 μM) upon addition of $CuSO_4$ and sodium ascorbate (SA). (E)

View Article Online
DOI: 10.1039/C7CC01093A
COMMUNICATION

Plot of PL intensity at 530 nm versus concentrations of TPEAzAl upon click reaction. (F) Size distributions of TPEAzAl before and after click reaction.

As TPEAzAl contains two azide and two alkyne groups on each molecule, it can automatically proceed with Cu^+ catalyzed click reaction to form AIE polymers with amplified fluorescence turn-on. To investigate the fluorescence change of TPEAzAl upon click reaction, the reaction was initiated by the addition of $CuSO_4$ and sodium ascorbate (SA) as the reducing agent.[13b] As shown in Figure 2D, the fluorescence increases gradually upon the initiation of click reaction, and saturates after 12 min of polymerization (Figure S14). The fluorescence intensity at 530 nm is ~23-fold stronger than its original emission after polymerization for 12 min. The fluorescence quantum yield before and after the polymerization of TPEAzAl was measured to be 0.005 and 0.18 by using quinoline sulfate as the standard. In addition, as shown in Figure 2E, after the click reaction, the PL intensities at 530 nm show a linear fitting line with its concentration (R^2 = 0.98), indicating that the click process can be monitored *via* the fluorescence change.

The underlying mechanism of click induced TPEAzAl fluorescence turn-on was further studied by DLS. As shown in Figure 2F, large aggregates of TPEAzAl were formed only with the addition of $CuSO_4$ and SA, which was confirmed by the tremendous increase in hydrodynamic diameters from less than 10 nm for TPEAzAl to above 1,000 nm after the click reaction. It should be noted that the sole addition of $CuSO_4$ or SA to TPEAzAl solution results in negligible size changes. The click polymerization induced aggregates formation was further confirmed by studying the fluorescence change of the click reaction product in water and DMSO mixture at different volume ratio. As shown in Figure S15, TPEAl is almost non-fluorescent in DMSO, while the fluorescence at f_{water} of 99% is very intense. However, for the click polymerized TPEAzAl, strong fluorescecnce are observed in both solvents. These results demonstrate that the fluorescence increase of TPEAzAl occures upon click polymerization. Both the polymerization and aggregation formation can restrict the molecular motions of TPEAzAl to turn-on its fluorescence in the polymer.

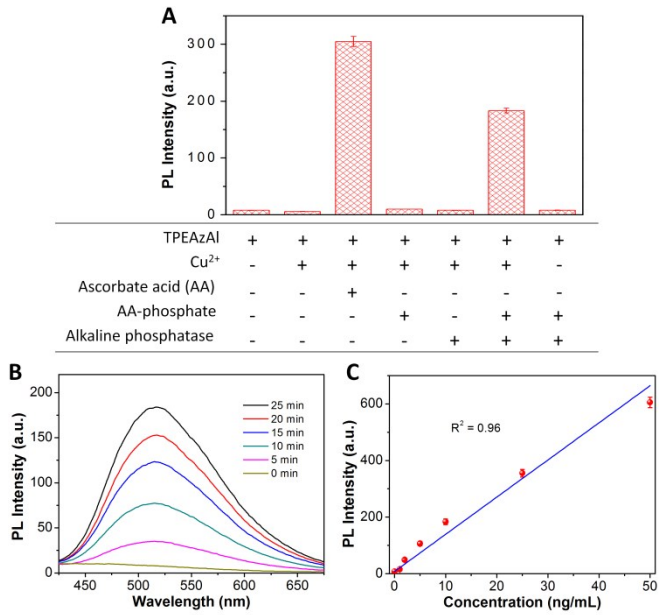

Figure 3. (A) PL intensity of TPEAzAl at 530 nm after the addition of Cu^{2+}, ascorbic acid, alkaline phosphatase or AA-phosphate; (B) Time-dependent PL spectra of TPEAzAl (10 μM) upon addition of Cu^{2+}, alkaline phosphatase and AA-phosphate; (C) Plot of PL intensity at 530 nm versus concentrations of alkaline phosphatase.

To produce a measurable signal in response to a binding event, antibody (or antigen) is often tethered to a detectable label such as an enzyme which can be quantified by a reaction with chromogenic/fluorogenic substrate. ALP is commonly involved in ELISA as the readout enzyme due to its good stability, broad substrate specificity, high turn-over number and commercial availability.[2c, 14] In traditional ELISA, the ALP activity is estimated by colorimetric measurement of dephosphorylates of chromogenic pNPP substrate. To explore the potential of using the click reaction induced fluorescence turn-on of TPEAzAl for monitoring ALP activity, we first studied the fluorescence response of TPEAzAl in the presence of AA-phosphate with or without the addition of ALP. ALP can transform AA-phosphate to the reducing agent AA through enzymatic reaction, which can reduce Cu^{2+} into Cu^+ to initiate the click reaction.[13a] As shown in Figure 3A, TPEAzAl shows strong fluorescence upon addition of both Cu^{2+} and AA, indicating the click reaction induced fluorescence turn-on. Faint fluorescence of TPEAzAl is observed after the addition of AA-phosphate or ALP alone. However, TPEAzAl shows strong fluorescence in the presence of AA-phosphate and ALP, indicating that AA-phosphate is dephosphorylated by ALP to form AA and acts as a reducing agent to generate Cu^+. Subsequent click reaction leads to the polymers that aggregates in solution with fluorescence turn-on. This is further confirmed by the negligible fluorescence change of TPEAzAl without the addition of Cu^{2+} in the presence of both AA-phosphate and ALP.

We also studied the time-dependent fluorescence change of TPEAzAl upon addition of Cu^{2+}, alkaline phosphatase and AA-phosphate. As shown in Figure 3B, the fluorescence intensifies gradually upon the initiation of the polymerization. After 25 min, the fluorescence intensity at 530 nm is about 23-fold higher than its original. The quick response rate enables the detection of ALP in a short time range. In addition, the fluorescence change at 530 nm of TPEAzAl with different concentrations of ALP ranging from 0 to 50 ng mL^{-1} was monitored. As shown in Figure 3C, the fluorescence intensities at 530 nm increase linearly with ALP concentrations in the range of 0−50 ng mL^{-1}. The results indicate that the fluorescence change of TPEAzAl can be used as a convenient signal for ALP sensing, which shows great potential for the development of ALP-based ELISA.

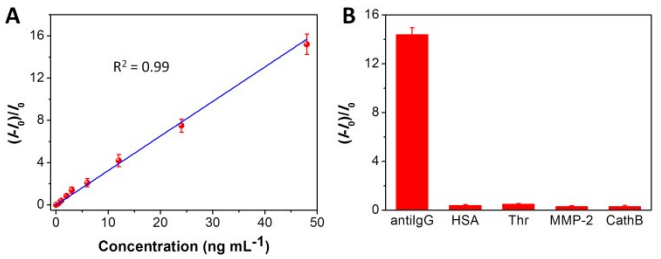

Figure 4. (A) PL intensity change of TPEAzAl at 530 nm at different concentrations of rabbit antihuman IgG. (B) Plot of $(I-I_0)/I_0$ for TPEAzAl upon incubation with different proteins, where I and I_0 are the PL intensities at protein concentrations of 50 and 0 ng mL^{-1}, respectively.

We further employed TPEAzAl as a fluorogenic substrate for ultrasensitive immunoassay to detect a model antibody, rabbit antihuman IgG. The procedure of fluorogenic ELISA in this study follows that of conventional ELISA. Specifically, human IgG as the antigen was first loaded on a 96-well plate and the target protein rabbit anti-human IgG as the primary antibody with different concentrations were immobilized through specific antigen-antibody interaction. After that, goat anti-rabbit IgG labeled with ALP as the secondary antibody was further immobilized. After washing away

the unbounded ALP-conjugated antibody, AA-phosphate, $CuSO_4$ and TPEAzAl were added to each well. We tested the concentrations of rabbit antihuman IgG ranging from 0 to 50 ng mL^{-1}. As shown in Figure 4A, the PL intensity of TPEAzAl at 530 nm intensifies gradually and fits linearly (R^2 = 0.99) to the concentration of target protein. Moreover, the limit of detection (LOD) for rabbit antihuman IgG based on this fluorogenic ELISA was estimated to be 1.2 ng mL^{-1}, which compares favorably with conventional ELISA using chromogenic pNPP as substrate. According to its standard protocols, the LOD of rabbit antihuman IgG was estimated to be 16.7 ng mL^{-1} based on the colorimetric change of pNPP substrate (Figure S16). In addition to the enhanced sensitivity, the high structural stability of TPEAzAl (no change in physical property and reactivity for at least 1-year storage) provides additional advantages of the fluorogenic assay. We also validated the specificity of this assay by testing a panel of commonly used proteins and enzymes that one could encounter in a typical biological application, including human serum albumin (HSA), thrombin (Thr), matrix metalloproteinases-2 (MMP-2) and cathepsin B (CathB). As shown in Figure 4B, only anti-IgG can initiate the click reaction and induce the fluorescence turn-on while other proteins exhibit no observable fluorescence intensity change. Therefore, the fluorescence turn-on is based on the specific immuno-reaction between antigen and antibody, rather than non specific interactions.

In summary, a fluorogenic ELISA has been developed for rabbit antihuman IgG detection. Water-soluble substrate TPEAzAl with two azide and two alykne groups was synthesized and its click reaction induced fluorescence turn-on was investigated. The ELISA using TPEAzAl as substrate exhibits significant advantages over conventional ELISA in terms of enhanced detection sensitivity and improved shelf life. Using rabbit antihuman IgG as a model, the detection limit based on the TPEAzAl substrate was estimated to be 1.2 ng mL^{-1}, which is 14 times more sensitive than that of conventional colorimetric assay using pNPP as substrate. This facile signal amplification strategy was achieved by the cascade dephosphorylate reaction of AA-phosphate to generate AA which reduced Cu^{2+} to Cu^{+} and subsequently initiated the click reaction of TPEAzAl to turn on the fluorescence. As the ALP-conjugated antibodies are widely used in the current ELISA platform, this signal amplification strategy fits within the existing ELISA technology, which can be easily extended to other analytes. It should be noted that although the current method shows high sensitivity, multiple processes involved would make it more sensitive to inhibitors or other interferences than the conventional assays. Overall, the conceptual integration of click reaction and AIE processes represent a promising strategy to the development of fluorogenic ELISA with optimized sensitivity and stability for biomedical diagnosis.

We thank Singapore NRF Investigatorship (R279-000-444-281), NRF CRP (R279-000-483-281), National University of Singapore (R279-000-482-133) and the Institute of Materials Research and Engineering, A-star of Singapore (IMRE/14-8P1110) for financial support.

Notes and references

[a]*Department of Chemical and Biomolecular Engineering, National University of Singapore,4 Engineering Drive 4, Singapore, 117585*
[b]*Institute of Materials Research and Engineering, Agency for Science, Technology and Research(A*STAR),3 Research Link, Singapore, 117602*
E-mail: cheliub@nus.edu.sg
‡These authors contribute equally.
†Electronic Supplementary Information (ESI) available: Detailed experimental methods and additional data. See DOI: 10.1039/b000000x/

1 (a) J. Kirsch, C. Siltanen, Q. Zhou, A. Revzin, A. Simonian, *Chem. Soc. Rev.* 2013, **42**, 8733-8768; (b) Y. Zhang, Y. Guo, Y. Xianyu, W. Chen, Y. Zhao, X. Jiang, *Adv. Mater.* 2013, **25**, 3802-3819; (c) J.-J. Xu, W.-W. Zhao, S. Song, C. Fan, H.-Y. Chen, *Chem. Soc. Rev.* 2014, **43**, 1601-1611.
2 (a) E. Engvall, P. Perlmann, *Immunochemistry*, 1971, **8**, 871-874; (b) S. S. Pierangeli, E. N. Harris, *Nat. protoc.* 2008, **3**, 840-848; (c) J. Shen, Y. Li, H. Gu, F. Xia, X. Zuo, *Chem. Rev.* 2014, **114**, 7631-7677.
3 (a) D. S. Hage, *Anal. Chem.* 1999, **71**, 294-304; (b) P. D. Howes, S. Rana, M. M. Stevens, *Chem. Soc. Rev.* 2014, **43**, 3835-3853.
4 (a) Y. Meng, K. High, J. Antonello, M. W. Washabaugh, Q. Zhao, *Anal. biochem.* 2005, **345**, 227-236; (b) D. Tang, Y. Cui, G. Chen, *Analyst* 2013, **138**, 981-990; (c) A. B. Chinen, C. M. Guan, J. R. Ferrer, S. N. Barnaby, T. J. Merkel, C. A. Mirkin, *Chem. Rev.* 2015, **115**, 10530-10574; (d) N. Malashikhina, G. Garai-Ibabe, V. Pavlov, *Anal. Chem.* 2013, **85**, 6866-6870.
5 (a) T. Deng, J. S. Li, J. H. Jiang, G. L. Shen, R. Q. Yu, *Adv. Funct. Mater.* 2006, **16**, 2147-2155; (b) Y. Iizumi, T. Okazaki, Y. Ikehara, M. Ogura, S. Fukata, M. Yudasaka, *ACS appl. mater. & interfaces* 2013, **5**, 7665-7670.
6 J. Zhao, D. Yang, Y. Zhao, X. J. Yang, Y. Y. Wang, B. Wu, *Angew. Chem. Int. Ed.* 2014, **53**, 6632-6636.
7 S. Chen, Y. Hong, Y. Liu, J. Liu, C. W. Leung, M. Li, R. T. Kwok, E. Zhao, J. W. Lam, Y. Yu, *J. Am. Chem. Soc.* **2013**, *135*, 4926-4929.
8 Y. Liu, Y. Tang, N. N. Barashkov, I. S. Irgibaeva, J. W. Lam, R. Hu, D. Birimzhanova, Y. Yu, B. Z. Tang, *J. Am. Chem. Soc.* 2010, **132**, 13951-13953.
9 (a) M. Wang, X. Gu, G. Zhang, D. Zhang, D. Zhu, *Anal. Chem.* 2009, **81**, 4444-4449; (b) H. Shi, R. T. Kwok, J. Liu, B. Xing, B. Z. Tang, B. Liu, *J. Am. Chem. Soc.* 2012, **134**, 17972-17981; (c) Y. Yuan, R. T. Kwok, B. Z. Tang, B. Liu, *J. Am. Chem. Soc.* 2014, **136**, 2546-2554; (d) L. Peng, R. Wei, K. Li, Z. Zhou, P. Song, A. Tong, *Analyst* 2013, **138**, 2068-2072; (e) Y. Ding, L. Shi, H. Wei, *Chem. Sci.* 2015, **6**, 6361-6366; (f) X. Wang, J. Hu, G. Zhang, S. Liu, *J. Am. Chem. Soc.* 2014, **136**, 9890-9893; (g) A. Shao, Z. Guo, S. Zhu, S. Zhu, P. Shi, H. Tian, W. Zhu, *Chem. Sci.* 2014, **5**, 1383-1389; (h) F. Hu, Y. Huang, G. Zhang, R. Zhao, H. Yang, D. Zhang, *Anal. Chem.* 2014, **86**, 7987-7995; (i) Y. Yuan, S. Xu, X. Cheng, X. Cai, B. Liu, *Angew. Chem. Int. Ed.* 2016, **55**, 6457-6461.
10 (a) X. Xue, Y. Zhao, L. Dai, X. Zhang, X. Hao, C. Zhang, S. Huo, J. Liu, C. Liu, A. Kumar, *Adv. Mater.* 2014, **26**, 712-717; (b) W. Guan, W. Zhou, C. Lu, B. Z. Tang, *Angew. Chem. Int. Ed.* 2015, **54**, 15160-15164.
11 (a) J. Mei, N. L. Leung, R. T. Kwok, J. W. Lam, B. Z. Tang, *Chem. Rev.* 2015, **115**, 11718–11940; (b) Z. Zhao, B. He, B. Z. Tang, *Chem. Sci.* 2015, **6**, 5347-5365.
12 (a) R. T. Kwok, C. W. Leung, J. W. Lam, B. Z. Tang, *Chem. Soc. Rev.* 2015, **44**, 4228-4238; (b) Y. Yuan, C. Zhang, S. Xu, B. Liu, *Chem. Sci.* 2016, **7**, 1862-1866; (c) J. Liang, B. Z. Tang, B. Liu, *Chem. Soc. Rev.* 2015, **44**, 2798-2811; (d) A. Shao, Y. Xie, S. Zhu, Z. Guo, S. Zhu, J. Guo, P. Shi, T. D. James, H. Tian, W. H. Zhu, *Angew. Chem. Inter. Ed.* 2015, **54**, 7275-7280; (e) X. Zhang, X. Zhang, L. Tao, Z. Chi, J. Xu, Y. Wei, *J. Mater. Chem. B* 2014, **2**, 4398-4414.
13 (a) T. Kuwahara, T. Homma, M. Kondo, M. Shimomura, *Biosens. and Bioelectron.* 2011, **26**, 3382-3385; (b) H. C. Kolb, M. Finn, K. B. Sharpless, *Angew. Chem. Int. Ed.* 2001, **40**, 2004-2021.
14 C. Ruan, Y. Li, *Talanta* 2001, **54**, 1095-1103.